

All you need is feedback: Communication with block attention feedback codes

Emre Ozfatura, Yulin Shao, Alberto Perotti, Branislav Popovic, Deniz Gündüz

Abstract

Deep learning based channel code designs have recently gained interest as an alternative to conventional coding algorithms, particularly for channels for which existing codes do not provide effective solutions. Communication over a feedback channel is one such problem, for which promising results have recently been obtained by employing various deep learning architectures. In this paper, we introduce a novel learning-aided code design for feedback channels, called *generalized block attention feedback (GBAF) codes*, which i) employs a modular architecture that can be implemented using different neural network architectures; ii) provides order-of-magnitude improvements in the probability of error compared to existing designs; and iii) can transmit at desired code rates.

Index Terms

I. INTRODUCTION

Designing communication systems that can best exploit feedback from the receiver has been an ongoing challenge over decades [1]–[13]. The formulation involves a transmitter-receiver pair connected via a forward and a feedback channel, and the goal is to reliably deliver a block of bits from the transmitter to the receiver. Shannon early on proved that the forward channel capacity is not increased by feedback [1], but feedback does improve the reliability of transmissions; that is, the error probability can be made to vanish faster with the blocklength. In this context, the central quest of feedback-aided channel coding is how to devise an efficient coding scheme to realize ultra-reliable communications by minimizing the block error rate (BLER). Such codes can have a significant impact on a variety of applications that require ultra-reliable short-packet communications [14], such as autonomous vehicles, industrial automation and control, tactile Internet, and augmented/virtual reality, to count a few.

Existing feedback codes can be classified as human-crafted codes [2], [3], [5], [7]–[9] and deep learning (DL)-aided codes [10]–[13]. Among human-crafted codes, two notable works are the SK scheme [2], [3], [6] and the modulo-SK scheme [9] designed for additive white Gaussian noise (AWGN) channels with noiseless and noisy feedback, respectively. The essence of these two schemes is describing the block of bits by a 2^K -ary pulse-amplitude modulation (PAM) constellation, where K is the block length, and transmitting the constellation point corresponding to the message iteratively over many interactions, where each interaction consists of one forward and one feedback transmission. At each interaction, the transmitter first recovers the receiver’s estimate of the constellation point, thanks to the feedback signal, and transmits a signal to correct the estimation error in the next interaction.

A main disadvantage of the human-crafted codes is that they are much sensitive to the numerical precision and quantization errors [6], [8], [10], [13]. Since the message is mapped to a 2^K -ary PAM constellation, the number of bits required to represent all the statistics in this process grows linearly with K . When K is large, these schemes suffer from severe quantization errors caused by the finite-precision arithmetic and finite quantization levels of the electronic parts and components, e.g., power amplifier (PA) and field-programmable gate array (FPGA) chip.

Emre Ozfatura, Yulin Shao and Deniz Gündüz are with Information Processing and Communications Lab, Department of Electrical and Electronic Engineering, Imperial College London Email: {m.ozfatura, y.shao, d.gunduz} @imperial.ac.uk.

A. Perotti and B. Popovic are with the Radio Transmission Technology Lab, Huawei Technologies Sweden AB, Kista 164-94, Sweden Email: {alberto.perotti, branislav.popovic}@huawei.com

On the other hand, DL-aided feedback codes model the communication system as an autoencoder [10]–[13], in which the encoder and decoder are modeled as a pair of deep neural networks (DNNs), while the wireless channel is treated as an untrainable stochastic layer. The code is obtained by end-to-end unsupervised learning to minimize the reconstruction error of the block of bits at the receiver.

Compared with human-crafted codes, DL-based feedback codes do not suffer from the constraint of finite precision and quantization level. Moreover, they are very flexible and can be easily trained for different scenarios. Specifically, both the SK and modulo-SK schemes are designed for the setup of unit-time delayed feedback and AWGN channels with a specific pair of feedforward and feedback signal-to-noise ratios (SNRs). In contrast, DL-based codes can be easily generalized to more practical setups [10], [13], such as feedback with greater delays, block feedback, and fading channels. On the other hand, existing DL-aided feedback codes suffer from the following limitations that we address in this paper:

- *Communication overhead:* In practice, each distinct use of the forward and feedback channels introduce a certain level of overhead and additional delay independent of the number of bits transmitted. We define the corresponding communication overhead as the number of ‘switches’ at the source node, between transmitting parity symbols and receiving feedback symbols, equivalently the number communication blocks T . In the previous designs, T linearly scales with K . One of our key objectives is to reduce this communication overhead without sacrificing the performance significantly.
- *Limited set of feasible rates:* Existing schemes are limited to code rates of $1/k, k \in \mathbb{Z}^+$. Hence, another important aspect of this work is to present a design that can transmit at a wider range of rates. The flexibility in the communication rate is important to achieve higher spectral efficiencies, particularly in the higher SNR regimes.
- *Lack of structure:* Existing codes are defined through the employed DNN architecture. Instead, we would like to provide a holistic view of the problem and introduce a generalized modular design, where modules can be added/removed, and implemented through arbitrary architectures addressing different requirements in terms of performance and complexity.

In this paper, we introduce the generalized black attention feedback (GBAF) code, which addresses all of the aforementioned limitations of existing designs. Moreover, by employing a transformer-based encoder architecture as its core sequence-to-sequence encoder module, GBAF codes achieve order of magnitude improvements in terms of the BLER performance over the whole range of channel SNRs compared to existing DL-based codes in the literature. Apart from [9], feedback codes in the literature are designed for a passive feedback scenario; that is, the feedback signal is simply a noisy version of the signal received at the receiver. While we also consider passive feedback in this paper, our design can be easily extended to active feedback. Next, we present the problem formulation in Section II. The structure and modules of the GBAF code is introduced in Section III. Numerical results illustrating its superiority are presented in Section IV. We conclude the paper in Section V.

II. PROBLEM DEFINITION

A. Notation

We use bold, capital bold, and capital calligraphic fonts to denote vectors, matrices, and sets, respectively, i.e., \mathbf{v} , \mathbf{V} , and \mathcal{V} . We use the notation $\mathbf{v}_{[\]}$, $\mathbf{V}_{[\]}$ to denote index slicing. Finally, we use the superscript for a vector/matrix/list to refer to its realization at a particular time/iteration.

B. Preliminaries

We focus on a point-to-point communication scenario with one transmitter and one receiver. The objective of the transmitter is to send K bits of information, $\mathbf{b} = [b_1, \dots, b_K] \in \{0, 1\}^K$, to the receiver in N channel uses. We impose a rate constraint of R , that is we must have $N \leq K/R$. Here, we use $\mathbf{c} = [c_1, \dots, c_N] \in \mathbb{R}^N$ to denote the sequence of transmitted symbols over the forward channel. We

model both the forward and feedback channels as additive white Gaussian noise (AWGN) channels with independent noise terms.

We consider a *block* feedback model; that is, the transmitter transmits a block of symbols, after which it receives a block of feedback symbols corresponding to the transmitted block over the forward channel. This model would be particularly relevant in the active feedback scenario, where the feedback symbols are encoded by the receiver. In the case of passive feedback considered in this paper, we use this model to quantify the potential overheads due to processing the feedback symbols and generating the transmitted symbols over the forward channel based on the received feedback signals. In the literature, this is assumed instantaneous; that is, the channel output feedback, noiseless or noisy, is assumed to be available instantly at the encoder. However, in practice, these feedback symbols need to be encoded and/or modulated as well, and in general, encoding/ decoding operations, as well as additional exchange of control information between the transmitter and receiver for every forward and feedback packet will introduce additional overheads. Hence, in practice, it is desired to utilize feedback with minimum overhead.

Let τ denote the index of the communication block. In communication block τ , the transmitter sends a block of N_τ symbols, denoted by $\mathbf{c}^{(\tau)}$, in the forward direction, and receives a block of N_τ symbols¹, denoted by $\tilde{\mathbf{y}}^{(\tau)}$, over the feedback link, for $\tau = 1, \dots, T-1$. The communication is terminated when the receiver receives $\mathbf{c}^{(T)}$. The received vector of symbols at the forward and feedback links, denoted by $\mathbf{y}^{(\tau)}$ and $\tilde{\mathbf{y}}^{(\tau)}$, respectively, are given by

$$\mathbf{y}^{(\tau)} = \mathbf{c}^{(\tau)} + \mathbf{n}^{(\tau)}, \quad \text{for } \tau = 1, \dots, T, \quad (1)$$

and,

$$\tilde{\mathbf{y}}^{(\tau)} = \mathbf{y}^{(\tau)} + \tilde{\mathbf{n}}^{(\tau)}, \quad \text{for } \tau = 1, \dots, T-1 \quad (2)$$

where $\mathbf{n}^{(\tau)}, \tilde{\mathbf{n}}^{(\tau)} \in \mathbb{R}^{N_\tau}$ are the noise vectors consisting of independent and identically distributed (i.i.d.) zero-mean Gaussian random variables with variances σ_{ff}^2 and σ_{fb}^2 , respectively.

The rate constraint, which limits the number of channel uses in the forward direction translates into the following inequality, $\sum_{\tau=1}^T N_\tau \leq N$. We remark that often the existing schemes, as well as proposed design, utilizes equal length blocks over τ , where a slight modification appears in the systematic code design which we explain later.

If we consider T communication blocks at forward direction, this also implies that the direction of communication is changed T times as well, thus describe the overhead of the feedback mechanism. As mentioned above, larger T corresponds to more overhead.

The focus of our research, similarly to the previous works, is to design a mechanism for generating symbols in forward and feedback directions for each communication block τ . Before describing the encoding mechanism, we introduce the so-called ‘knowledge vectors’ $\mathbf{q}^{(\tau)}$ and $\tilde{\mathbf{q}}^{(\tau)}$, which refer to all the available information at the transmitter and receiver ends, respectively, when generating the symbols transmitted in communication block τ . The knowledge vector at the transmitter $\mathbf{q}^{(\tau)}$, consist of the original bit stream, and the previously transmitted symbols and the received feedback symbols up to time τ , i.e.,

$$\mathbf{q}^{(\tau)} = [\mathbf{b}, \mathbf{c}^{(1)}, \dots, \mathbf{c}^{(\tau-1)}, \tilde{\mathbf{y}}^{(1)}, \dots, \tilde{\mathbf{y}}^{(\tau-1)}]. \quad (3)$$

Similarly, the knowledge vector at the receiver is given by

$$\tilde{\mathbf{q}}^{(\tau)} = [\mathbf{y}^{(1)}, \dots, \mathbf{y}^{(\tau)}]. \quad (4)$$

Let $M^{(\tau)}$ denote the encoding function at the transmitter. We have

$$M^{(\tau)} : \mathbf{q}^{(\tau)} \rightarrow \mathbf{c}^{(\tau)} \in \mathbb{R}^{N_\tau}. \quad (5)$$

¹In general, in the active feedback scenario, we can have different number of symbols transmitted over each block of the forward and feedback channels. Here, we set them to be equal as we assume that the symbols transmitted over the feedback channel are simply the symbols received at the receiver.

Once the transmission of all the symbols are completed, a decoding function D is employed at the receiver to recover the original bit stream, i.e.,

$$D : \tilde{\mathbf{q}}^{(T)} \rightarrow \hat{\mathbf{b}} \in \{0, 1\}^K. \quad (6)$$

The overall communication protocol must satisfy an average power constraint on the transmitted symbols:

$$\mathbb{E} \left[\frac{1}{N} \sum_{\tau=1}^T \langle \mathbf{c}^{(\tau)}, \mathbf{c}^{(\tau)} \rangle \right] \leq 1. \quad (7)$$

$$(8)$$

Hence, we have a SNR of $SNR_{ff} = 1/\sigma_{ff}^2$ in the forward direction and $SNR_{fb} = 1/\sigma_{fb}^2$ in the feedback direction. We refer to the case $\sigma_{fb} = 0$ as *noiseless feedback*.

1) *Systematic Feedback*: We refer to a feedback code as a *systematic feedback code*, if at $\tau = 1$, the encoder at the transmitter maps the original bit stream to its BPSK modulated version, i.e., $N_1 = K$, and

$$M^{(1)} : \mathbf{q}^{(1)} = \mathbf{b} \xrightarrow{\text{BPSK}} \mathbf{c}^{(1)} = \bar{\mathbf{b}} = 2 * \mathbf{b} - 1, \quad (9)$$

Although, we have restricted the definition above to BPSK modulated symbols for the sake of simplicity, the same notion can be extended to other modulation schemes with larger constellations. In general, there is no particular reason to restrict ourselves to a systematic feedback node, but we explicitly defined this set of codes as the DL-based codes considered in the literature [10]–[12] are all systematic codes.

C. DNN-Based Feedback Codes

DNN-based feedback codes utilize neural architectures for encoding parity symbols at the transmitter and decoding received symbols at the receiver. That is, the encoding and decoding mappings, M and D , respectively, are implemented as DNN architectures. We first revisit some of the existing feedback code designs in the literature and illustrate how they are operated according to our generic framework. First of all, the common aspects of the existing strategies, the DeepCode [10], the DEF code [11], and the DRF code [12], is that they consider systematic and passive feedback schemes. Therefore, the overall communication process is divided into two phases corresponding to $\tau = 1$ and $\tau > 1$, respectively. $M^{(1)}$ is the modulation scheme described in (9). In the second phase, $\tau > 1$, a NN architecture denoted by H_{encoder} is used as the encoder to generate the vector of parity symbols, i.e., we have

$$H_{\text{encoder}} : S_{\text{encoder}}(\mathbf{q}^{(\tau)}) \xrightarrow{\text{Neural-encoder}} \mathbf{c}^{(\tau)}, \quad (10)$$

where $S_{\text{encoder}}(\cdot)$ denotes the pre-processing function that defines how the knowledge vector $\mathbf{q}^{(\tau)}$ is fed to the DNN architecture H_{encoder} . To be more precise, often, DNN-based encoder architectures accept inputs in the form of sequence of vectors, thus the $S_{\text{encoder}}(\cdot)$ is used to transform the knowledge vector into a particular form fed to the encoder.

Another common aspect in the previous architectures is that, at the second phase in each communication block, exactly two symbols are transmitted, i.e., $q_\tau = 2$ for all $\tau > 1$. Accordingly, for given K and R , in total $T = \frac{K}{2} * \left(\frac{1}{R} - 1\right) + 1$ communication blocks are transmitted in the forward direction². Similarly, at the receiver a combination of DNN architecture H_{decoder} and pre-processing function $S_{\text{decoder}}(\cdot)$ is used as a decoder D , i.e.,

$$H_{\text{decoder}} : S_{\text{decoder}}(\tilde{\mathbf{q}}^{(T)}) = [\mathbf{y}^{(1)}, \dots, \mathbf{y}^{(T)}] \rightarrow \hat{\mathbf{b}} \in \{0, 1\}^K. \quad (11)$$

The psrticular DNN architectures used, both as encoder and decoder, in the codes in the literature are listed in Table I.

²To prevent any confusion, we ignore the extra zero padding strategy [10]

Design	H_{decoder}	H_{encoder}
DeepCode [10]	Bi-GRU	GRU [15]
DRFC [12]	Bi-LSTM	LSTM [16]
AttentionCode [13]	Transformer Encoder	Transformer Encoder [17]

TABLE I: DNN-based designs for feedback codes.

III. GENERALIZED BLOCK ATTENTION FEEDBACK (GBAF) CODES

The core idea behind the proposed GBAF code design is to divide K original information bits into l blocks of m bits each, $K = l \cdot m$; and hence, to have a sequence of l vectors. We then utilize sequence-to-sequence encoding by using a transformer architecture to generate the parity bits to be transmitted, and update the sequence of vectors with the symbols received over the feedback channel, by appending them to the corresponding block. A total of $N_\tau = l = K/m$ symbols, one parity symbol for each block, are transmitted at each iteration τ . One can observe that, given rate R and block size m , the number of required communication blocks is $T = m/R$, which does not scale with K . Furthermore, by choosing different $T \in \mathbb{Z}^+$ and $m \in \mathbb{Z}^+$ values it is possible to obtain wide range rate values $R = m/(T)$. Hence, the rate of the code can be adjusted by changing the block size m and the number of communication blocks which is also equivalent to number of parity symbols per block.

In order to provide a more holistic view from the design perspective, we present the GBAF code design in three parts: the architecture, modules employed, and implementation.

A. Architecture

From the operational point of view, we employ two types of components in the overall design, namely an encoder unit and a pre-processing unit. Motivated by the SK scheme [2], the transmitter consists of two cascaded blocks, each of which consists of a pre-processing unit followed by an encoder unit. We refer to the initial block as the *belief network* and the latter as the *parity network*. The objective of the belief network is to generate a belief on the predicted bits at the receiver, while the objective of the *parity network* is to generate parity symbols to improve the prediction accuracy at the receiver. The receiver also employs a single block with the same structure to predict the original bit stream, which we refer as the decoder network. Accordingly, the overall architecture consists of three feedback mechanisms; namely, *inner feedback*, *outer feedback* and *belief feedback*, which we explain next:

Inner Feedback: We use the term inner feedback to refer to a feedback mechanism within each block. It is used for the encoder network to recall the previously generated parity symbols.

Belief Feedback: The belief feedback is the directed communication link between the belief network and the encoder network.

Outer Feedback: The outer feedback is the physical feedback signals from the receiver to the transmitter. The overall framework is illustrated in Fig. 1. In the introduced framework, belief network and belief feedback are optional, that is, they can be added or removed as desired, and the objective of using two networks is to disentangle the task of generating parity bits and predicting the belief at the target node. However, by bypassing the belief network and disabling the belief feedback both tasks can be fulfilled by the parity network.

B. Modules

In the GBAF code, for all the encoder units we utilize the same DNN architecture denoted with H_{encoder} , which simply maps sequences of l vectors of size d_{in} to sequences of vectors of size d_{out} with the same length, i.e.,

$$H_{\text{encoder}} : \mathcal{Q} = (\mathbf{q}_1, \dots, \mathbf{q}_l) \xrightarrow{\text{Encoding}} \mathcal{V} = (\mathbf{v}_1, \dots, \mathbf{v}_l),$$

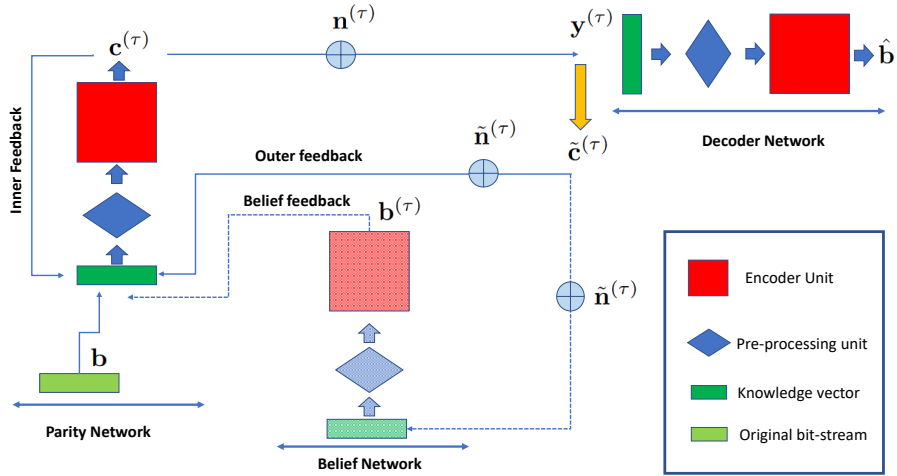


Fig. 1: Illustration of the overall GBAF code architecture. The green, blue and red blocks denote the knowledge vector, pre-processing unit and encoder unit, respectively. The dashed lines and shapes indicate the units and connections that are optional.

such that $\mathbf{q}_i \in \mathbb{R}^{d_{in}}$, $\mathbf{v}_i \in \mathbb{R}^{d_{out}}$. H_{encoder} unit consists of three modules, in the following order from bottom to top, feature extractor H_{extract} , sequence-to-sequence encoder H_{s2s} , output mapping H_{map} . Accordingly, $H_{\text{encoder}} = H_{\text{map}} \circ H_{s2s} \circ H_{\text{extract}}$, where \circ denotes composition.

1) *Feature extractor*: The role of the feature extractor is to map the collected raw data for each block to a certain vector representation similar to the vector embedding approach in NLP tasks [18]–[20], where the objective is to represent the words in the form of a vector and the corresponding representation inherits certain contextual information regarding the word. However, our problem has two unique challenges: 1) time-evolving nature of data; 2) the randomness in the data. By the randomness, we refer to the random noise realization at each communication block. In principle, encoder module utilizes the noise realizations to generate parity symbols, nevertheless, the outlier noise realizations, particularly in the low SNR regime, might be overemphasized when a simple linear mapping is used for feature extraction. Hence, our ultimate aim is to design a feature extractor module in a way that the impact of each raw data on the corresponding representation is limited. To this end, we utilize a multi-layer perceptron (MLP) architecture with Gaussian error linear unit (GELU) activation [21]. As shown in Fig. 3 of Appendix A, the feature extractor consists of three linear layers with two GELU activation functions [21] in between.

2) *Sequence-to-sequence Encoder*: In a broad sense sequence-to-sequence encoder H_{s2s} is a DNN architecture, where the sequence of early feature representations are mapped to sequence of final latent representation by seeking certain correlation among them. The input to the H_{s2s} is a sequence of d_{model} dimensional vectors of length l and the output is a sequence of d_{out} dimensional vectors of length l . Hence, wide range of existing NN architectures, particularly those employed for NLP such LSTM, GRU, transformer, can be utilized as H_{s2s} . We have observe that transformer architecture is particularly perform well in the scope of our problem. Hence, for H_{s2s} we consider sequence of N encoder layers of the transformer architecture³, which consists of three main components: feed forward module, multi-head attention module, and layer normalization module. Further details on these modules please refer to [17] and [22]. In our implementation we consider $d_{\text{model}} = 32$, single attention head, and $4 \times$ scaling at the feedforward module following the common implementation [22], and finally for the layer normalization we follow the pre-layer normalization option [23]. For the number of encoder layers N , we consider $N_{\text{parity}} = 2$, $N_{\text{belief}} = 2$ and $N_{\text{decoder}} = 3$.

³We follow the standard implementation used in the Pytorch library: https://pytorch.org/docs/stable/_modules/torch/nn/modules/transformer.html#TransformerEncoderLayer

Algorithm 1 Unified iterative parity symbol encoding (UIPSE)

```

1: for  $\tau = 1, \dots, T$  do # Generate 1 parity symbol per block at each pass
2:   Update knowledge vector:
3:    $\mathbf{q}^{(\tau)} = [\mathbf{b}, \mathbf{c}^{(1)}, \dots, \mathbf{c}^{(\tau)}, \tilde{\mathbf{y}}^{(1)}, \dots, \tilde{\mathbf{y}}^{(\tau-1)}]$ 
4:   if Belief feedback is enabled then
5:     Pre-process knowledge vector for belief network:
6:      $\{\tilde{\mathbf{q}}_i^{(\tau)}, \dots, \tilde{\mathbf{q}}_l^{(\tau)}\} = S_{\text{belief}}(\mathbf{q}^{(\tau)}), \tilde{\mathbf{q}}_i^{(\tau)} = [\tilde{\mathbf{y}}_i^{(1)}, \dots, \tilde{\mathbf{y}}_i^{(\tau-1)}]$ 
7:     Extract features:  $\tilde{\mathbf{f}}_i^{(\tau)} = H_{\text{extract}}^{\text{belief}}(\tilde{\mathbf{q}}_i^{(\tau)})$ 
8:     Attention-based neural-encoding:  $\mathcal{V}^{(\tau)} = H_{\text{encoder}}^{\text{belief}}(\tilde{\mathcal{F}}^{(\tau)})$ 
9:     Generate belief feedback:  $\mathbf{b}_i^{(\tau)} = H_{\text{map}}^{\text{belief}}(\tilde{\mathbf{v}}_i^{(\tau)})$ 
10:    Pre-process knowledge vector:  $\{\mathbf{q}_i^{(\tau)}, \dots, \mathbf{q}_l^{(\tau)}\} = S_{\text{parity}}(\mathbf{q}^{(\tau)}, \mathbf{b}^{(\tau)})$ 
11:  else
12:    Pre-process knowledge vector:  $\{\mathbf{q}_i^{(\tau)}, \dots, \mathbf{q}_l^{(\tau)}\} = S_{\text{parity}}(\mathbf{q}^{(\tau)})$ 
13:  Feature extraction:
14:  for  $i \in [l]$  do  $\mathbf{f}_i^{(\tau)} = H_{\text{extract}}^{\text{parity}}(\mathbf{q}_i^{(\tau)})$ 
15:  Attention-based neural-encoding:  $\mathcal{V}^{(\tau)} = H_{s2s}^{\text{parity}}(\mathcal{F}^{(\tau)})$ 
16:  Symbol mapping:
17:  for  $i \in [l]$  do
18:     $c_i^{(\tau)} = H_{\text{map}}^{\text{parity}}(\mathbf{v}_i^{(\tau)})$  # Generate 1 parity symbol as feedback for  $i$ th block

```

3) *Output Mapping:* The output mapping H_{map} is used to map the final latent representing, obtained by sequence-to-sequence encoder H_{s2s} , to a particular form based on use purpose, that is, in parity network H_{map} is used to map final representation to parity symbol, whereas in belief network and decoder it is used for the classification purposes. The common aspect of H_{map} in all three networks, it consist of single FC layer with input size of d_{model} and output size of d_{out} , however when it used for the classification purpose, as in belief and decoder network, FC is followed by additional softmax layer. Since, one parity symbol is generated per block, we consider $d_{\text{out}} = 1$ for $H_{\text{map}}^{\text{parity}}$. On the other hand, decoder network aim to map each block to one of the 2^m possible m length bit stream. Hence, for $H_{\text{map}}^{\text{parity}}$ we consider $d_{\text{out}} = 2^m$. Finally, for belief network $H_{\text{map}}^{\text{belief}}$, we set $d_{\text{out}} = 2m$, that is for each original bit in the block we generate two values in order to denote likelihood values $P(b_i = 0)$ and $P(b_i = 1)$ as a belief, using softmax layer⁴. Finally, we note here that due to the average power constraint, an extra layer for power normalization is required following the $H_{\text{map}}^{\text{parity}}$ and we follow the same procedure in [10], [13].

C. Implementation

Here, we illustrate how the proposed GBAF code design is executed from the algorithmic view in order to highlight the its iterative aspect. To describe the overall encoding process at the source node, we introduce an iterative algorithm called unified iterative parity symbol encoding (UIPSE), that generates l symbols each communication block, which is illustrated in Algorithm 1.

To describe the final decoding mechanism in target node, we introduce the joint parity symbol decoder (JPSD) algorithm, where parity symbols belong to each block are decoded jointly, as illustrated in Algorithm 2. Different from the existing feedback code designs, due to use of block structure, the decoder perform classification over all possible blocks, 2^m in total, rather than binary classification. Hence, to recover the original bit-stream we further employ a lookup-table \mathbf{A} (line 16-18 in Algorithm 2), such that the i th row of \mathbf{A} , $\mathbf{A}_{[i,:]}$, corresponds to the bit-wise representation of the i th possible block.

⁴Here, we remark that before the softmax operation we reshape the input, i.e., $1 \times 2m \rightarrow m \times 2$.

Algorithm 2 Joint parity symbol Decoding (JPSD)

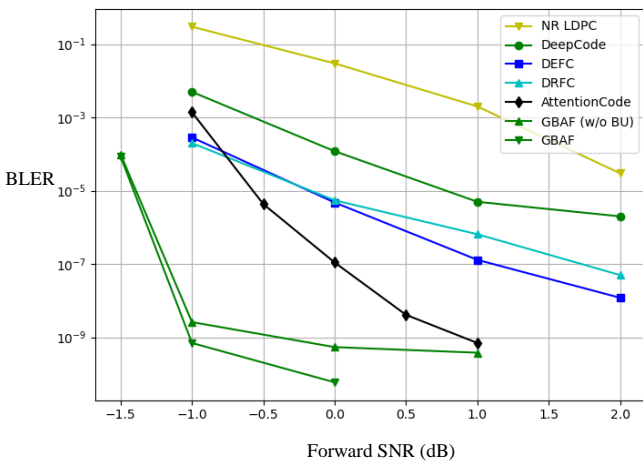
- 1: **Update Knowledge vector:**
 - 2: $\hat{\mathbf{q}} = [\tilde{\mathbf{c}}^{(1)}, \dots, \tilde{\mathbf{c}}^{(T-1)}, \mathbf{y}^{(1)}, \dots, \mathbf{y}^{(T)}]$
 - 3: **Pre-process knowledge vector for decoder network:**
 - 4: $S_{\text{decoder}}(\hat{\mathbf{q}}) = \{\hat{\mathbf{q}}_1, \dots, \hat{\mathbf{q}}_l\}, \quad \hat{\mathbf{q}}_i = [\tilde{\mathbf{y}}_i^{(1)}, \dots, \tilde{\mathbf{y}}_i^{(T)}]$
 - 5: **Feature extraction:**
 - 6: **for** $i \in [l]$ **do** $\hat{\mathbf{f}}_i = H_{\text{extract}}^{\text{decoder}}(\hat{\mathbf{q}}_i)$
 - 7: **Attention-based neural-encoding:** $\hat{\mathbf{v}} = H_{s2s}^{\text{decoder}}(\hat{\mathcal{F}})$
 - 8: **Mapping:**
 - 9: **for** $i \in [l]$ **do** $\mathbf{w}_i = H_{\text{map}}^{\text{decoder}}(\hat{\mathbf{v}}_i)$
 - 10: **Block-wise classification:** # predict the block index
 - 11: **for** $i \in [l]$ **do** $p_i = \max_j(\mathbf{w}_i)_{[j]}$
 - 12: **Block index to bit stream conversion:** # map block indices to original bits
 - 13: **for** $i \in [l]$ **do** $\tilde{\mathbf{b}} = [\tilde{\mathbf{b}}, \mathbf{A}_{[p_i, :]}]$
-

IV. NUMERICAL RESULTS

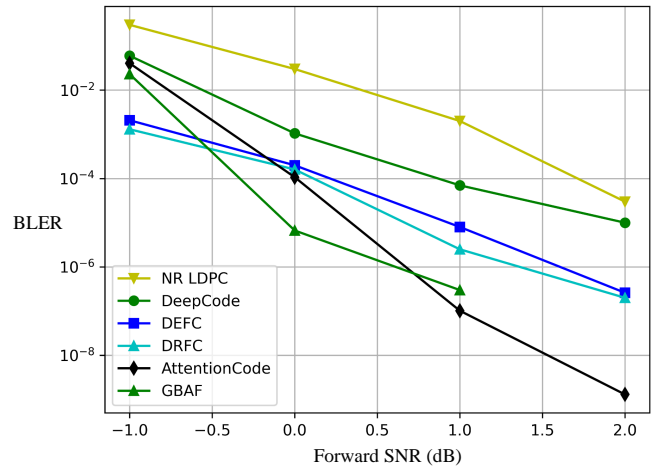
A. Experiment Setup

In all the experiments, we consider a bit stream of length $K = 51$ and a block size of $m = 3$, such that the number of blocks is $l = 17$. We consider $SNR_{ff} \in [-1, 2]$ dB, and the transmission of $T = 9$ parity bits for each block in total, which corresponds to a transmission rate of $R = 3/9$.

For the training, we utilized the AdamW optimizer, which is a variation of the Adam optimizer with decoupled weight decay regularization [24]. We consider a batch size of $B = 8192$, the initial learning rate of 0.001, and a weight decay parameter 0.01. In addition, we apply gradient clipping with threshold 0.5. We train the network for 100K batches using cross-entropy loss and apply polynomial decay to the learning rate. Following the previous works, we consider the block length error rate (BLER) as a performance metric for our analysis. We conduct our experiments under two different scenarios namely, noisy and noiseless feedback.



(a) BLER performance versus the forward channel SNR (in dB). The feedback channel is noiseless.



(b) BLER performance versus the forward channel SNR (in dB). The feedback channel SNR is 20 dB.

Fig. 2: Performance comparison of GBAF with AttentionCode, DEFC, DRFC, DeepCode and NR-LDPC

TABLE II: Performance of GBAF codes with different communication rates; $R = 3/8, 3/7, 3/6, 3/5$.

SNR/Rate	3/8	3/7	3/6	3/5
-1 dB	1.8×10^{-2}	-	-	-
0 dB	5.5×10^{-6}	1.2×10^{-2}	-	-
1 dB	2.7×10^{-8}	7.5×10^{-7}	1×10^{-2}	-
2 dB	2.5×10^{-9}	1.2×10^{-7}	1.5×10^{-6}	6.5×10^{-2}
3 dB	-	1.4×10^{-9}	1.4×10^{-7}	3×10^{-6}

B. Experimental Results

We start our analysis with the noiseless feedback scenario i.e., $\sigma_{fb}^2 = 0$. In the first part of the simulation we focus fixed the transmission rate to $R = 3/9$, and compare the proposed design with the existing NN-based feedback designs DeepCode [10], DEFC [11], DRFC [12], AttentionCode [13] as well as LDPC code enhanced with neural decoder. In the first part of the simulations, we examine two variations of GBAF code based on appearance of belief network in order to highlight its impact on the performance. The BLER performance results are illustrated in Fig. 2(a) for the forward SNR values in the range of $[-1, 2]$ dB. The results clearly highlights that GBAF code achieves order of magnitude improvements compared to the best performing counterpart. We also observe that use of belief network further improves the performance. Nevertheless, design of the feature extraction module become more critical when the belief network is employed, and we observe that the belief network with the introduced feature extraction module may not be effective for the noisy feedback scenario. For now, we consider their joint design as an open research problem and in the remaining simulations we disable the belief network for GBAF code.

In the second part of the simulations we have highlighted the rate adaptive nature of the proposed GBAF code, that is, unlike the existing design, the proposed framework can be also utilized for higher rates. To this end, we consider $T = 8, 7, 6, 5$ to achieve the rates $R = 3/8, 3/7, 3/6, 3/5$, and measure the BLER performance for forward SNR values in the range of $[-1, 3]$, which is illustrated in Table II.

The results demonstrate that when operating under higher SNR regimes, it is possible to achieve acceptable BLER target with higher rates. To be more precise, considering 10^{-5} as BLER target, which is sufficient for several tasks [14], then the target can be achieved with rates $R = 3/8, 3/7, 3/6, 3/5$ for $SNR_{ff} = 0, 1, 2, 3$ dB, respectively. Hence, GBAF code is more desirable due to its flexibility for rate adaptation based on the SNR.

Now we consider the scenario where the feedback channel is also exposed to additive Gaussian noise with $1/\sigma_{fb}^2 = 20$ dB. The illustrated results in Fig 2(b) indicates that except the lowest SNR value of -1 dB, GBAF code outperforms the alternatives DeepCode, DRFC, DEFC. We also observe that at higher SNR values AttentionCode may outperform the GBAF code. However, we highlight the fact that GBAF code utilizes the feedback less frequently, approximately $6\times$ less, compared to the counterparts to minimize the overhead.

C. Further Discussions

The performance comparison between AttentionCode and GBAF code illustrates that, the performance gain achieved by the GBAF code is not only related to the chosen sequence-to-sequence encoder architecture but also the way it is implemented. Besides, compared to the AttentionCode implementation, GBAF code reduces the computational complexity and the memory requirement since the use of blocks induce a reduction, linearly proportional to the block-size, on the sequence length. Since the computational complexity of transformer architecture is $\mathcal{O}(l^2)$, although there are recent works targeting linear complexity [25]–[27], this implies $m^2\times$ reduction on the complexity, which makes GBAF codes practical for longer block lengths as well. We also remark that existing solutions transmits exactly two parity symbols at each communication block, thus for $R = 3/9$ $T = 52$, whereas with GBAF $T = 9$, which implies a significant reduction on the overhead. Finally, we remark that by utilizing curriculum learning scheme used in [13],

the BLER performance can be improved further, especially for higher SNR values where we observe certain saturation on the BLER performance.

V. CONCLUSION

In this work, we have introduced the generalized block attention feed back architecture (GBAF), which empowered by sequence-to-sequence encoding NN architectures, particularly transformer architecture, to generate parity bits, by incorporating a feedback mechanism, bits for error correction purposes. Beyond introducing a generic framework, unlike the existing solutions described through the employed NN architecture, the proposed framework also address several practical limitations of the existing solution and make NN-based feedback codes more applicable for the next generation networks. Finally, in addition to all these advantages, we have also shown that GBAF code significantly outperforms the existing solutions, especially in the noiseless feedback scenario.

APPENDIX

A. Details on the pre-processing unit

The pre-processing unit of the encoder network can be operated under four different mode based on the enabled/disabled feedback mechanisms and the way the available information are aggregated. In Algorithm 3, we illustrate pre-processing mechanism under each mode with different color. In our implementation, we prefer the third option illustrated with blue. Here, we also note that in our implementation we store the original bits \mathbf{b} in the knowledge vector in the BPSK modulated form, i.e., $\bar{\mathbf{b}} = 2 * \mathbf{b} - 1$. In overall, with enable/disable option for the belief network the GBAF code design can be operated under 8 different modes as highlighted in Algorithm 3.

Algorithm 3 Pre-processing unit for Parity Network: $S_{parity}()$

```

1: if Belief  $\mathbf{b}^{(\tau)}$  is available then
2:   if Feedback only is True then
3:      $\mathbf{q}_i^{(\tau)} = [\mathbf{b}_{((i-1)*m+1:i*m)}, \mathbf{b}_i^{(\tau)}, \tilde{\mathbf{y}}_i^{(1)}, \dots, \tilde{\mathbf{y}}_i^{(\tau-1)}]$ 
4:   else if Noise only is True then
5:      $\mathbf{q}_i^{(\tau)} = [\mathbf{b}_{((i-1)*m+1:i*m)}, \mathbf{b}_i^{(\tau)}, \tilde{\mathbf{y}}_i^{(1)} - \mathbf{c}_i^{(1)}, \dots, \tilde{\mathbf{y}}_i^{(\tau-1)} - \mathbf{c}_i^{(\tau-1)}]$ 
6:   else if Disentangle is True then
7:      $\mathbf{q}_i^{(\tau)} = [\mathbf{b}_{((i-1)*m+1:i*m)}, \mathbf{b}_i^{(\tau)}, \mathbf{c}_i^{(1)}, \dots, \mathbf{c}_i^{(\tau-1)}, \tilde{\mathbf{y}}_i^{(1)} - \mathbf{c}_i^{(1)}, \dots, \tilde{\mathbf{y}}_i^{(\tau-1)} - \mathbf{c}_i^{(\tau-1)}]$ 
8:   else
9:      $\mathbf{q}_i^{(\tau)} = [\mathbf{b}_{((i-1)*m+1:i*m)}, \mathbf{b}_i^{(\tau)}, \mathbf{c}_i^{(1)}, \dots, \mathbf{c}_i^{(\tau-1)}, \tilde{\mathbf{y}}_i^{(1)}, \dots, \tilde{\mathbf{y}}_i^{(\tau-1)}]$ 
10: else
11:   if Feedback only is True then
12:      $\mathbf{q}_i^{(\tau)} = [\mathbf{b}_{((i-1)*m+1:i*m)}, \tilde{\mathbf{y}}_i^{(1)}, \dots, \tilde{\mathbf{y}}_i^{(\tau-1)}]$ 
13:   else if Noise only is True then
14:      $\mathbf{q}_i^{(\tau)} = [\mathbf{b}_{((i-1)*m+1:i*m)}, \tilde{\mathbf{y}}_i^{(1)} - \mathbf{c}_i^{(1)}, \dots, \tilde{\mathbf{y}}_i^{(\tau-1)} - \mathbf{c}_i^{(\tau-1)}]$ 
15:   else if Disentangle is True then
16:      $\mathbf{q}_i^{(\tau)} = [\mathbf{b}_{((i-1)*m+1:i*m)}, \mathbf{c}_i^{(1)}, \dots, \mathbf{c}_i^{(\tau-1)}, \tilde{\mathbf{y}}_i^{(1)} - \mathbf{c}_i^{(1)}, \dots, \tilde{\mathbf{y}}_i^{(\tau-1)} - \mathbf{c}_i^{(\tau-1)}]$ 
17:   else
18:      $\mathbf{q}_i^{(\tau)} = [\mathbf{b}_{((i-1)*m+1:i*m)}, \mathbf{c}_i^{(1)}, \dots, \mathbf{c}_i^{(\tau-1)}, \tilde{\mathbf{y}}_i^{(1)}, \dots, \tilde{\mathbf{y}}_i^{(\tau-1)}]$ 

```

B. Feature extractor

The feature extractor consists of three linear layers with two Gaussian error linear unit (GELU) activation functions [21] in between, as shown in Fig. 3. With this design, we hope the GELU activation function can truncate noise realizations with a large amplitude such that these large, but very rare noise realizations does not affect the learning process.

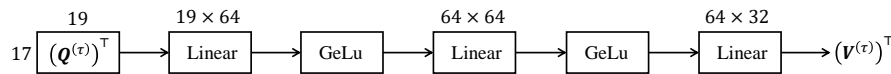


Fig. 3: Feature extractor for noise suppression, where `dim_in` is determined by the chosen pre-processing mode in Algorithm 3.

REFERENCES

- [1] C. Shannon, “The zero error capacity of a noisy channel,” *IRE Trans. Inf. Theory*, vol. 2, no. 3, pp. 8–19, 1956.
- [2] J. Schalkwijk and T. Kailath, “A coding scheme for additive noise channels with feedback i: No bandwidth constraint,” *IEEE Trans. Inf. Theory*, vol. 12, no. 2, pp. 172–182, 1966.
- [3] J. Schalkwijk, “A coding scheme for additive noise channels with feedback ii: Band-limited signals,” *IEEE Trans. Inf. Theory*, vol. 12, no. 2, pp. 183–189, 1966.
- [4] K. Zigangirov, “Upper bounds for the error probability for channels with feedback,” *Problemy Peredachi Informatsii*, vol. 6, no. 2, pp. 87–92, 1970.
- [5] N. C. Martins and T. Weissman, “Coding for additive white noise channels with feedback corrupted by quantization or bounded noise,” *IEEE Trans. Inf. Theory*, vol. 54, no. 9, pp. 4274–4282, 2008.
- [6] R. G. Gallager and B. Nakiboğlu, “Variations on a theme by schalkwijk and kailath,” *IEEE Trans. on Inf. Theory*, vol. 56, no. 1, pp. 6–17, 2009.
- [7] Z. Chance and D. J. Love, “Concatenated coding for the awgn channel with noisy feedback,” *IEEE Trans. Inf. Theory*, vol. 57, no. 10, pp. 6633–6649, 2011.
- [8] Y.-H. Kim, A. Lapidoth, and T. Weissman, “The gaussian channel with noisy feedback,” in *IEEE ISIT*, 2007, pp. 1416–1420.
- [9] A. Ben-Yishai and O. Shayevitz, “Interactive schemes for the awgn channel with noisy feedback,” *IEEE Trans. Inf. Theory*, vol. 63, no. 4, pp. 2409–2427, 2017.
- [10] H. Kim, Y. Jiang, S. Kannan, S. Oh, and P. Viswanath, “Deepcode: Feedback codes via deep learning,” *IEEE Journal on Selected Areas in Information Theory*, vol. 1, no. 1, pp. 194–206, 2020.
- [11] A. R. Safavi, A. G. Perotti, B. M. Popovic, M. B. Mashhadi, and D. Gunduz, “Deep extended feedback codes,” 2021.
- [12] M. B. Mashhadi, D. Gündüz, A. Perotti, and B. M. Popovic, “DRF codes: Deep snr-robust feedback codes,” *CoRR*, vol. abs/2112.11789, 2021. [Online]. Available: <https://arxiv.org/abs/2112.11789>
- [13] Y. Shao, M. Ozfatura, D. Gunduz, A. Perotti, and B. Popovic, “Attentioncode: short-packet ultra-reliable communications with feedback for 6G,” 2022.
- [14] M. Shirvanimoghaddam, M. S. Mohammadi, R. Abbas, A. Minja *et al.*, “Short block-length codes for ultra-reliable low latency communications,” *IEEE Commun. Magazine*, vol. 57, no. 2, pp. 130–137, 2018.
- [15] K. Cho, B. van Merriënboer, D. Bahdanau, and Y. Bengio, “On the properties of neural machine translation: Encoder-decoder approaches,” *CoRR*, vol. abs/1409.1259, 2014. [Online]. Available: <http://arxiv.org/abs/1409.1259>
- [16] H. Sak, A. W. Senior, and F. Beaufays, “Long short-term memory based recurrent neural network architectures for large vocabulary speech recognition,” *CoRR*, vol. abs/1402.1128, 2014. [Online]. Available: <http://arxiv.org/abs/1402.1128>
- [17] A. Vaswani, N. Shazeer, N. Parmar, J. Uszkoreit, L. Jones, A. N. Gomez, L. u. Kaiser, and I. Polosukhin, “Attention is all you need,” in *Advances in Neural Information Processing Systems*, I. Guyon, U. V. Luxburg, S. Bengio, H. Wallach, R. Fergus, S. Vishwanathan, and R. Garnett, Eds., vol. 30. Curran Associates, Inc., 2017. [Online]. Available: <https://proceedings.neurips.cc/paper/2017/file/3f5ee243547dee91fbd053c1c4a845aa-Paper.pdf>
- [18] J. Pennington, R. Socher, and C. D. Manning, “Glove: Global vectors for word representation,” in *Proceedings of the 2014 conference on empirical methods in natural language processing (EMNLP)*, 2014, pp. 1532–1543.
- [19] A. Bordes, N. Usunier, A. Garcia-Duran, J. Weston, and O. Yakhnenko, “Translating embeddings for modeling multi-relational data,” in *Advances in Neural Information Processing Systems*, C. Burges, L. Bottou, M. Welling, Z. Ghahramani, and K. Weinberger, Eds., vol. 26. Curran Associates, Inc., 2013. [Online]. Available: <https://proceedings.neurips.cc/paper/2013/file/1cecc7a77928ca8133fa24680a88d2f9-Paper.pdf>
- [20] T. Mikolov, I. Sutskever, K. Chen, G. Corrado, and J. Dean, “Distributed representations of words and phrases and their compositionality,” 2013.
- [21] D. Hendrycks and K. Gimpel, “Gaussian error linear units (gelus),” *arXiv preprint arXiv:1606.08415*, 2016.
- [22] J. Devlin, M. Chang, K. Lee, and K. Toutanova, “BERT: pre-training of deep bidirectional transformers for language understanding,” *CoRR*, vol. abs/1810.04805, 2018. [Online]. Available: <http://arxiv.org/abs/1810.04805>
- [23] R. Xiong, Y. Yang, D. He, K. Zheng, S. Zheng, C. Xing, H. Zhang, Y. Lan, L. Wang, and T. Liu, “On layer normalization in the transformer architecture,” *CoRR*, vol. abs/2002.04745, 2020. [Online]. Available: <https://arxiv.org/abs/2002.04745>
- [24] I. Loshchilov and F. Hutter, “Decoupled weight decay regularization,” in *International Conference on Learning Representations*, 2019. [Online]. Available: <https://openreview.net/forum?id=Bkg6RiCqY7>
- [25] N. Kitaev, L. Kaiser, and A. Levskaya, “Reformer: The efficient transformer,” *CoRR*, vol. abs/2001.04451, 2020. [Online]. Available: <https://arxiv.org/abs/2001.04451>
- [26] S. Wang, B. Z. Li, M. Khabsa, H. Fang, and H. Ma, “Linformer: Self-attention with linear complexity,” *CoRR*, vol. abs/2006.04768, 2020. [Online]. Available: <https://arxiv.org/abs/2006.04768>
- [27] K. Choromanski, V. Likhoshesterov, D. Dohan, X. Song, A. Gane, T. Sarlós, P. Hawkins, J. Davis, A. Mohiuddin, L. Kaiser, D. Belanger, L. J. Colwell, and A. Weller, “Rethinking attention with performers,” *CoRR*, vol. abs/2009.14794, 2020. [Online]. Available: <https://arxiv.org/abs/2009.14794>